

Article

Experimental Evaluation of the Properties of Asphalt Binders Modified with Calcium Sulfate Anhydrous Whiskers and Polyester Fibers

Taotao Fan ^{1,2}, Chundi Si ^{1,2,*} and Junfeng Gao ³ 

¹ School of Traffic and Transportation, Shijiazhuang Tiedao University, Shijiazhuang 050043, China; fantaotao@stdu.edu.cn

² State Key Laboratory of Mechanical Behavior and System Safety of Traffic Engineering Structures, Shijiazhuang Tiedao University, Shijiazhuang 050043, China

³ National & Local Joint Engineering Laboratory of Transportation and Civil Engineering Materials, Chongqing Jiaotong University, Chongqing 400074, China; jfgao@cqjtu.edu.cn

* Correspondence: sichundi@stdu.edu.cn

Abstract: The use of waste calcium sulfate whiskers in pavement construction is cost-effective and beneficial to the environment. In this paper, modified asphalt binders are prepared by adding calcium sulfate anhydrous whiskers (ACSW, 9 wt.%, 11 wt.%, and 13 wt.% by weight of asphalt binder) and polyester fibers (4 wt.%, 6 wt.%, and 8 wt.% by weight of asphalt binder). The viscosity-temperature, rheological, and low-temperature properties of the modified asphalt binder were evaluated using the Brookfield rotational viscosity test, the dynamic shear rheometer (DSR) test, the bending beam rheometer (BBR) test, and the force ductility test. The results demonstrated that the addition of the ACSW and polyester fiber could improve the anti-deformation and low-temperature properties of the asphalt binders, but reduce their viscosity-temperature properties to some extent. The modified asphalt binder with 11 wt.% ACSW and 8% polyester fiber showed the best anti-deformation property, while the 11 wt.% ACSW and 6 wt.% polyester fiber modified asphalt binder had a better low-temperature performance. The force ductility test was more suitable than the BBR test to characterize the low-temperature properties of the modified asphalt binders. The Fourier-transform infrared spectroscopy (FTIR) and scanning electron microscope (SEM) tests were conducted to study the functional groups and micro-structure of the modified asphalt binders, and the results indicated that no new functional groups were generated and that the interaction between the ACSW, polyester fiber, and asphalt binder was a physical adsorption and interleaving process.

Keywords: calcium sulfate anhydrous whisker; polyester fiber; modified asphalt binder; road properties; micro-structure



Citation: Fan, T.; Si, C.; Gao, J. Experimental Evaluation of the Properties of Asphalt Binders Modified with Calcium Sulfate Anhydrous Whiskers and Polyester Fibers. *Coatings* **2023**, *13*, 1802. <https://doi.org/10.3390/coatings13101802>

Academic Editor: Valeria Vignali

Received: 21 September 2023

Revised: 16 October 2023

Accepted: 19 October 2023

Published: 20 October 2023



Copyright: © 2023 by the authors. Licensee MDPI, Basel, Switzerland. This article is an open access article distributed under the terms and conditions of the Creative Commons Attribution (CC BY) license (<https://creativecommons.org/licenses/by/4.0/>).

1. Introduction

Calcium sulfate anhydrous whisker (ACSW) is a type of calcium sulfate whisker that comes from calcium salt and gypsum [1–3]. As an eco-friendly material, ACSWs are widely applied in terms of composite materials [4–7], owing to their advantageous properties of high-modulus and high-temperature anti-deformation. L. Xu et al. found that the anhydrous micron CaSO₄ improved the mechanical abilities of PVC [8]. J.F. Lou et al. proved that it was feasible to combine two-dimensional lamellar anhydrous calcium sulfate and polyethylene glycol to prepare a nanocomposite phase change material [9].

In pavement engineering, calcium sulfate whiskers are used to improve the performance of road materials [10,11]. K. Cao et al. evaluated the mechanical properties and microstructure of calcium-sulfate-whisker-modified cement-based composites. The results showed that the calcium sulfate whisker enhanced the tensile and anti-fracture properties of the cement-based composites by generating ettringite and whisker pullout, crack-bridging

at their micro-structure [12]. Y. Xu et al. evaluated that calcium sulfate whiskers could enhance the high-temperature and water stability of an asphalt mixture and that the mixture's water stability would reach its best performance when the dosage level of the calcium sulfate whiskers was 0.4%, but the calcium sulfate whiskers' impact on bettering the mixture's low-temperature quality was not obvious [13]. G.Y. Li et al. found that ACSWs decreased the temperature-sensitivity of a modified asphalt binder while increasing its high-temperature and viscosity-temperature properties [14]. T.T. Fan et al. investigated the high- and low-temperature, rheological, and viscosity-temperature properties of ACSWs based on the DSR, BBR, and Brookfield rotational viscosity tests. The authors found that, when the contents of ACSW ranged from 7 wt.% to 11 wt.%, the high-temperature and rheological properties of the asphalt were obviously enhanced, while, on the contrary, their temperature-sensitivity and low-temperature properties were weakened [15,16]. To overcome the disadvantage of ACSWs on the low-temperature properties of asphalt binders, it is necessary to develop a compound-modified asphalt binder.

Adding two or more types of modifiers with excellent qualities is an adequate means to improve the properties of asphalt pavement materials. These modifiers mainly involve natural, synthetic-organic, and inorganic materials, such as fibers, whiskers, high-molecular polymers, rubber, or other materials [17,18]. X.Y. Xing et al. evaluated that the composite of nano- CaCO_3 particles, CaCO_3 whiskers, and aramid fibers could enhance the high-temperature properties of asphalt binders [19]. According to the conventional indicator tests and DSR test, Rana A. Yousif et al. found that both recycled brown wool fiber and Chinese polyester fiber could strengthen the rheological quality of an asphalt binder and that the fiber types and dosage levels had an obvious influence on its high-temperature quality [20]. The results of ZH. Fu et al.'s study implied that basalt fiber and nano- TiO_2/ZnO could strengthen the high-temperature resistance of asphalt binders. After mixing in the basalt fiber, the low-temperature quality of the asphalt binder was lowered, and the negative effect from the addition of the fiber could be alleviated after adding in nano- TiO_2/ZnO [21]. Y.T. Liu et al. investigated the performance of an asphalt mixture modified with ACSW and waste cooking oil and found that the 6% ACSW and 2% waste cooking oil-modified mixture had better high- and low-temperature properties [22]. T.T. Fan et al. found that the 11.84% ACSW and 0.4% polyester fiber-modified asphalt mixture had the best hydrothermal performance and could meet the requirements for use in hot-humid, rainy regions [23]. Previous research showed that fibers could reinforce the qualities of asphalt binders by building a three-dimensional cross-linked structure and light component sorption of asphalt [24,25]. Therefore, it was of engineering importance to analyze the impact of mixing asphalt binder with ACSWs and fibers on the asphalt's characteristics.

Polyester fibers are widely used in asphalt pavement materials and play a significant role in improving the high- and low-temperature performances of asphalt binders. In this research, ACSWs and polyester fibers were selected to prepare the modified asphalt binder. The viscosity-temperature, rheological, and low-temperature properties of the ACSW and polyester fiber composite-modified asphalt binder (APMA) were analyzed through the Brookfield rotational viscosity test, the DSR test, the BBR test, and the force ductility test, respectively. The functional groups and micro-structure of the APMA were researched using the Fourier-transform infrared spectroscopy (FTIR) and Scanning electron microscope (SEM) tests. The study's processes were organized as follows. Firstly, ACSW and polyester fiber compound-modified asphalt binders with different proportions were prepared. Secondly, the viscosity-temperature, rheological, and low-temperature performances of the modified asphalt binders were evaluated. At last, the interaction mechanism between the ACSW-polyester fiber composite and the asphalt binder was analyzed. To take control of any experimental results' mistakes, three parallel examinations were conducted in each experiment. These results would then serve as a reference for future research on the ACSW and polyester fiber compound modification techniques and applications in asphalt pavements.

2. Materials and Methods

2.1. Materials

2.1.1. Base Asphalt Binder

The SK-90# asphalt binder (penetration grade: 80/100) (Shaanxi Changda Huachu Engineering Materials Technology Co., Ltd., Xi'an, China) was chosen, and its basic physical characteristics are listed in Table 1.

Table 1. Physical properties of the asphalt binder.

Test	Softening Point	Ductility at 10 °C	Penetration at 25 °C	Penetration Index
Unit	°C	cm	0.1 mm	-
Results	46.5	>100	85.9	-0.083
Method	ASTM D36	ASTM D113		ASTM D5

2.1.2. ACSW

The basic properties of the ACSW (Zhengzhou Bokeli Ecological Engineering Co., Ltd., Zhengzhou, China) used in this research were the average aspect ratios of 40–100, the average lengths of 10–200 µm, and the melting point of 1450 °C. The contents of ACSWs were 9 wt.%, 11 wt.%, and 13 wt.% of the base asphalt binder's mass.

2.1.3. Polyester Fiber

The physical properties of the polyester fiber (Changzhou Tianyi Engineering Fiber Co., Ltd., Changzhou, China) were a length of 6 mm, an average diameter of 10–20 µm, and a melting point of 259 °C. The amounts of polyester fiber were 4 wt.%, 6 wt.%, and 8 wt.% of the base asphalt binder's mass.

2.2. Methods

2.2.1. Preparation of the Composite-Modified Asphalt Binder

The ACSW and polyester fiber were mixed with the SK-90# asphalt binder at the temperature of 170 ± 3 °C for 30 min at the rotation rate of 400 rpm using a DJ1C-200 booster electric mixer.

2.2.2. Brookfield Rotational Viscosity Test

A Brookfield rotational viscosity test was carried on to evaluate the viscosity–temperature characteristics of the APMAs. Based on ASTM D4402 [26], the viscosity values of the APMAs were measured under different temperatures (90, 110, 135, 155, and 175 °C). The rotation rate was 20 r/min, and the rotor type was 21#. The viscosity–temperature characteristic index (*VTS*) was conducted as Equation (1) to estimate the viscosity–temperature properties of the APMAs.

$$\lg \lg(\eta \times 10^3) = A - VTS \lg(T) \quad (1)$$

where η stands for viscosity, measured in Pa·s; T stands for experimental temperature, measured in °C; and A is the equation's constant.

2.2.3. DSR Test

According to AASHTO T315 [27], the rheological characteristics of the APMAs were researched using a DSR (H-PTD200). The sizes of the test samples were 25 mm in diameter and 1 mm in thickness. The test shear rate was 10 rad/s. The experimental parameters, complex shear modulus (G^*), and phase angle (δ) were gauged, and the rutting factor ($G^*/\sin\delta$) was calculated at the temperature of 58, 64, 70, 76, and 82 °C, respectively.

2.2.4. BBR Test

The crack-resistance performances of the APMAs under low temperatures was studied using the BBR test (Thermoelectric Bending-Beam, Cannon, Tokyo, Japan). Based on AASHTO

T313 [28], the test samples were prepared with a special mold, and their sizes were a growth of 127 ± 2.0 mm, a thickness of 6.35 ± 0.05 mm, and a width of 12.7 ± 0.05 mm. The applied load was constant (980 ± 50) MN; the temperature was -12 °C, and the whole test lasted for 4 min. The experimental parameters, creep stiffness (S) and m -value, were gauged to study the low-temperature characteristics of the APMAs.

2.2.5. Force Ductility Test

Previous research has evaluated that the force ductility test is an efficacious way to characterize the low-temperature property of a modified asphalt binder [29–32]. In this paper, the maximum tension and tensile work were measured to evaluate the low-temperature properties of the APMA using the force ductility test (LYY-10A-CL). The test's temperature and tensile rate were 5 °C and 5 cm/min, respectively.

2.2.6. Microscopic Test

The chemical composition of the APMA was evaluated using FTIR (Nicolet Nexus 670, Thermo Fisher Scientific, Waltham, MA, USA). The experimental parameters were as follows: 500–4000 cm^{-1} wave numbers, 4 cm^{-1} resolution, and 16 scanning times.

The micro-structure of the APMA was implied using SEM (Hitachi S4800, Tokyo, Japan) and the electron beam voltage was 2.0 kv.

3. Results and Discussion

3.1. Viscosity-Temperature Characteristic

3.1.1. The Viscosity at 135 °C

The Brookfield rotational viscosity test results at 135 °C for the APMAs are shown in Figure 1. The 135 °C viscosity of the base asphalt binder was 0.344 Pa·s.

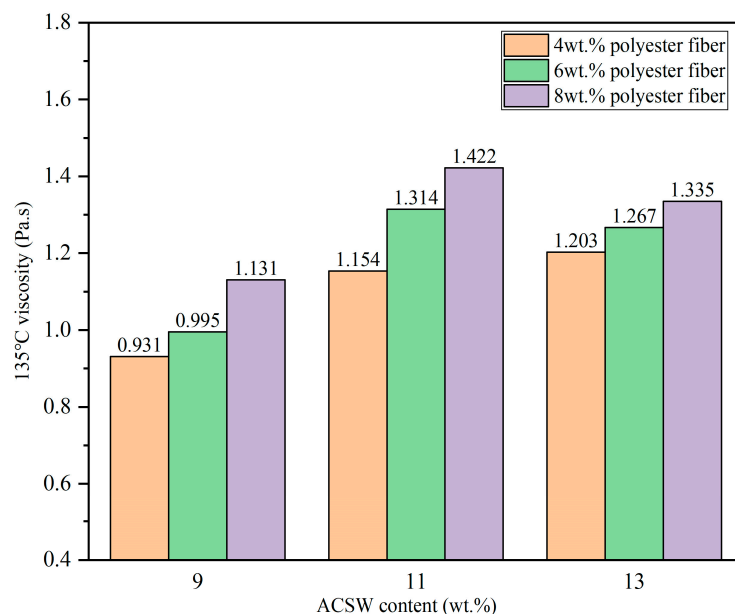


Figure 1. 135 °C viscosity results of the APMAs.

From Figure 1, due to the impact of the ACSW and polyester fiber, it could be seen that the values of the 135 °C viscosity of the modified asphalt binders were obviously enhanced. In detail, when the ACSW contents were kept constant, the 135 °C viscosity values of the APMAs gradually increased with the increase in polyester fiber contents. When the amount of polyester fiber was 4 wt.%, the 135 °C viscosity values of the APMAs increased with the increase in ACSW contents, and, when the amount of polyester fiber exceeded 4 wt.%, the 135 °C viscosity values of the APMAs first became larger and then lower with increasing ACSW dosages. The 135 °C viscosity values of the asphalt binder reached the

maximum value (1.422 Pa·s) after mixing with 11 wt.% ACSW and 8 wt.% polyester fiber. The results suggested that the modified asphalt binder had the best rheological properties when the contents of ACSW and PF were appropriate. The reason might be that, on the one hand, the light constituent of asphalt binder was adsorbed on the surfaces of the ACSW and polyester fiber, which increased the anti-slip force between the ACSW–polyester fiber composite and the asphalt binder; on the other hand, the polyester fiber was dispersed into a three-dimensional interweaving structure, enhancing the flow resistance of the APMA.

3.1.2. VTS

The Brookfield rotational viscosity test results of the modified asphalt binders under different temperatures are shown in Figure 2. The viscosity values of all the APMAs sharply decreased with the increase in test temperatures, which demonstrated that the APMAs had temperature-dependent properties. In detail, when the temperatures were changed from 90 °C to 135 °C, the viscosity values of the modified asphalt binders sharply reduced, and, when the temperatures were higher than 135 °C, the viscosity values of the modified asphalt binders slowly decreased. The reason for this might be that, as the temperature rises, the state of the asphalt binder changes from visco-elasticity to visco-plasticity, and the internal molecules and the frictional force gradually decline between the asphalt binder and ACSW–polyester fiber composite.

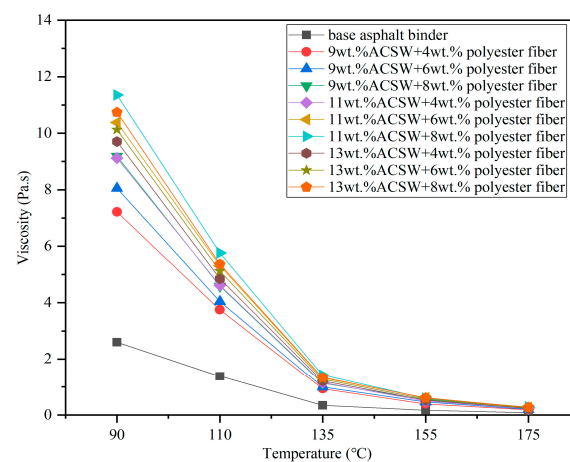


Figure 2. The viscosity results of the APMAs under different temperatures.

The viscosity–temperature performance of the asphalt binder was closely related to the construction technology of the asphalt mixture. Therefore, it was of great significance to study the viscosity–temperature performance of the APMAs to guide their application in asphalt pavements. In this paper, the *VTS* was adopted to evaluate the viscosity–temperature property of the APMAs; the *VTS* values of all the APMAs were calculated based on Equation (1), and the results are listed in Table 2. The *Adj.R-Square* values of all the regression equations were larger than 0.970, which implied that the regression equation had a good fit and could explore the relation between the temperature and viscosity of the APMA.

The larger the values of *VTS*, the greater the viscosity–temperature property of the APMA. From Table 2, the *VTS* values of the asphalt binders were reduced after adding the ACSW and polyester fiber. The results suggested that the ACSW and polyester fiber could cripple the viscosity–temperature properties of the asphalt binders. At the same ACSW content level, the *VTS* values of the APMA decreased with the increase in polyester fiber contents. In comparison to the base asphalt binder, the *VTS* values of the 4 wt.%, 6 wt.%, and 8 wt.% polyester fiber–modified asphalt binders showed a decrease of 9.12%, 11.06%, and 11.63%. Meanwhile, at the same polyester fiber content level, the *VTS* values of the APMA decreased with the increase in ACSW contents; namely, the *VTS* values of the 9 wt.%, 11 wt.%, and 13 wt.% ACSW–modified asphalt binders showed a decrease of 8.99%,

11.52%, and 11.4%. After adding 13 wt.% ACSW and 8 wt.% polyester fiber, the VTS value of the asphalt binder reached the minimum value (0.7652), which was reduced by 12.7% compared to that of the base asphalt binder.

Table 2. The VTS results of the APMAs.

ACSW Content (wt.%)	Polyester Fiber Content (wt.%)	Regression Equation	Adj.R-Square	VTS
0	0	$y = 2.2656 - 0.8770x$	0.9756	0.8770
9	4	$y = 2.1914 - 0.8120x$	0.9720	0.8120
9	6	$y = 2.1710 - 0.7994x$	0.9726	0.7994
9	8	$y = 2.1502 - 0.7856x$	0.9709	0.7856
11	4	$y = 2.1537 - 0.7876x$	0.9742	0.7876
11	6	$y = 2.1181 - 0.7664x$	0.9720	0.7664
11	8	$y = 2.1359 - 0.7733x$	0.9740	0.7733
13	4	$y = 2.1628 - 0.7907x$	0.9732	0.7907
13	6	$y = 2.1333 - 0.7748x$	0.9740	0.7748
13	8	$y = 2.1167 - 0.7652x$	0.9751	0.7652

3.2. Rheological Performance

3.2.1. The Results of G^* and δ

The influence of the ACSW and polyester fiber on the rheological performance of asphalt binder was analyzed using a complex shear modulus (G^*) and phase angle (δ), and the results of the DSR test are shown in Figures 3 and 4.

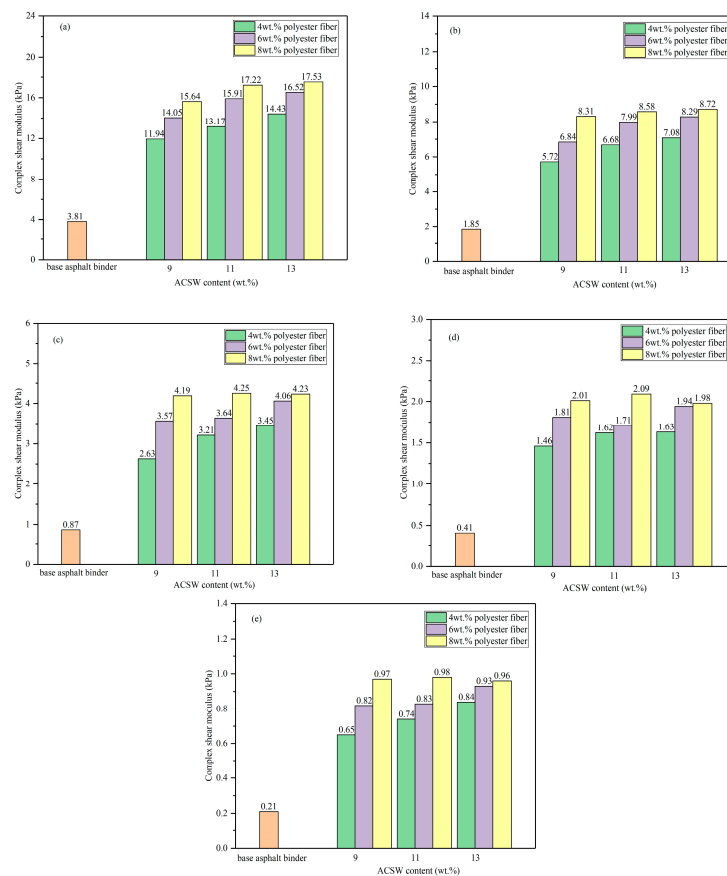


Figure 3. Complex shear modulus results of the APMAs under different temperatures. (a) 58 °C; (b) 64 °C; (c) 70 °C; (d) 76 °C; and (e) 82 °C.

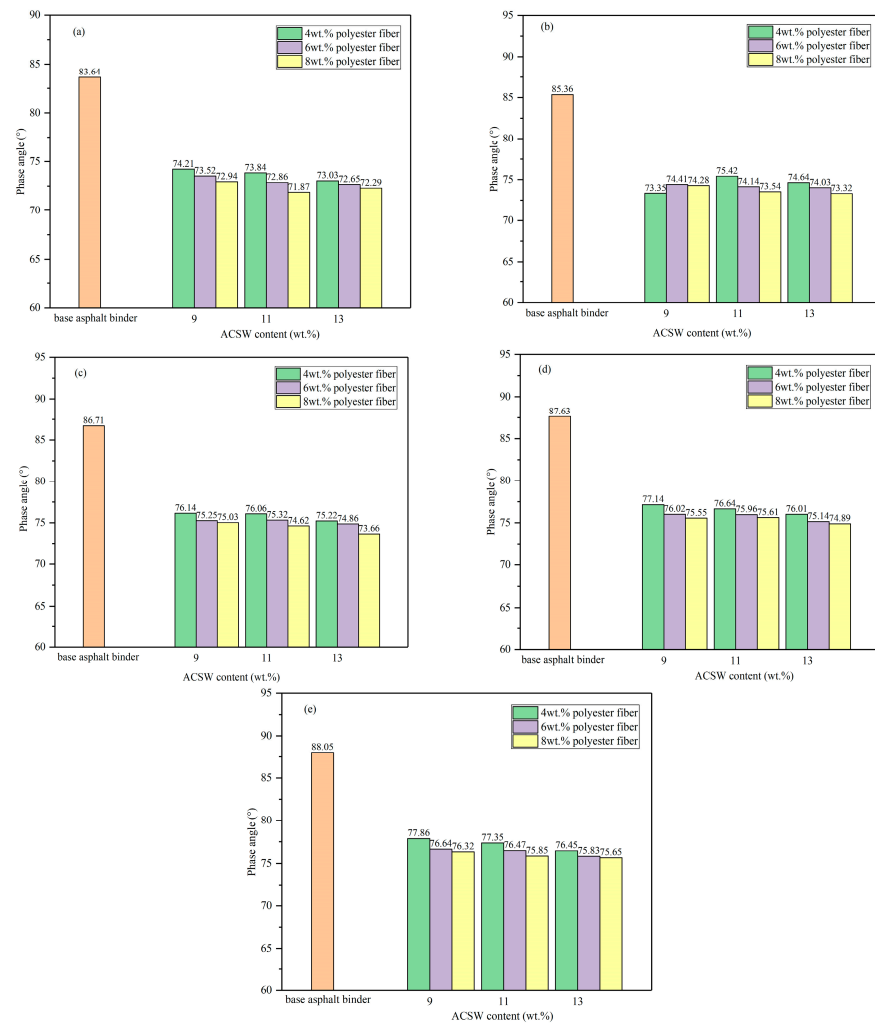


Figure 4. Phase angle results of the APMAs under different temperatures. (a) 58 °C; (b) 64 °C; (c) 70 °C; (d) 76 °C; and (e) 82 °C.

From Figure 3, when the temperature was kept constant, the G^* values of the asphalt binders increased with the increase in the amount of ACSW and polyester fiber. Under the same content level of ACSW, the G^* values of the modified asphalt binders increased with the increase in polyester fiber contents, and the analogous conclusion was made for the change of the G^* values of the APMA after adding the ACSW. The results implied that the ACSW and polyester fiber-compound modification would enhance the anti-deformation property of the asphalt binder.

The G^* values of the APMA reached their maximum value with 11 wt.% ACSW and 8 wt.% polyester fiber under different temperatures; namely, when the temperatures were 58, 64, 70, 76, and 82 °C, the maximum values of G^* for the APMA were 17.53 kPa (13 wt.% ACSW and 8 wt.% polyester fiber), 8.72 kPa (13 wt.% ACSW and 8 wt.% polyester fiber), 4.25 kPa (11 wt.% ACSW and 8 wt.% polyester fiber), 2.09 kPa (11 wt.% ACSW and 8 wt.% polyester fiber), and 0.98 kPa (11 wt.% ACSW and 8 wt.% polyester fiber). The results showed that the G^* values of the APMA sharply declined as the temperature increased and also proved that the modified asphalt binder had a significant temperature sensitivity.

Figure 4 implies that the δ values of all the APMA become larger as the temperature rises. The results evaluated that raising the temperature would enhance the fluidity of the asphalt binder. At the same temperature, the δ values of the asphalt binders decreased, at first, after adding the ACSW and polyester fiber and then, with the ACSW contents (or

polyester fiber contents) becoming larger, the δ values of all the APMAs were reduced. Taking the 11 wt.% ACSW and 8 wt.% polyester fiber-compound-modified asphalt binder as an example for analysis, when the temperatures were 58, 64, 70, 76, and 82 °C, the δ values of the asphalt binders were 71.87°, 73.54°, 74.62°, 75.61°, and 75.85°, while, in comparison to the base asphalt binder, the δ values of the asphalt binders decreased by 14.07%, 13.85%, 13.94%, 13.72%, and 13.86%.

Combined with the change in the values of G^* and δ , it was manifested that the elastic ingredients of the asphalt binder were enhanced, and its viscous components were reduced by raising the content levels of the ACSW and polyester fiber. The adsorption between the asphalt binder and the ACSW-polyester fiber resulted in the relative dosages of the elastic ingredient of the APMA being higher and those of the fluidity and plasticity components being lower.

3.2.2. Temperature Sensitivity

The temperature sensitivity of the asphalt binders was related to their deformation resistance, and a better temperature sensitivity of asphalt binders could improve the durability of asphalt pavement materials. To evaluate the influence of the ACSW and polyester fiber-compound modification on the temperature sensitivity of the asphalt binder, the statistical comparison between the slopes of the linear regression equations was executed based on Equation (2).

$$\lg \lg(G^* \times 10^3) = -GTS \times \lg T + K \quad (2)$$

where T stands for the experimental temperature, measured in °C; GTS and K stand for the regression coefficients.

The GTS results of the APMAs are listed in Table 3, and the larger the value of the GTS , the greater the temperature sensitivity of the asphalt binder.

Table 3. The GTS results of the APMAs.

ACSW Content (wt.%)	Polyester Fiber Content (wt.%)	Regression Equation	Adj.R-Square	GTS
0	0	$y = 2.774 - 1.254x$	0.9896	1.254
9	4	$y = 2.471 - 1.052x$	0.9875	1.052
9	6	$y = 2.387 - 0.999x$	0.9836	0.999
9	8	$y = 2.353 - 0.977x$	0.9832	0.977
11	4	$y = 2.444 - 1.033x$	0.9845	1.033
11	6	$y = 2.491 - 1.055x$	0.9881	1.055
11	8	$y = 2.389 - 0.995x$	0.9861	0.995
13	4	$y = 2.390 - 1.001x$	0.9871	1.001
13	6	$y = 2.394 - 0.999x$	0.9837	0.999
13	8	$y = 2.428 - 1.017x$	0.9873	1.017

From Table 3, the values of all Adj.R-Square were larger than 0.980, implying that Equation (2) could be used to fit the relation between the values of G^* and the temperature of the APMAs.

The GTS values of all the APMAs were lower than that of the base asphalt binder, which demonstrated that the ACSW and polyester fiber could weak the temperature sensitivity of the asphalt binder. In contrast to the base asphalt binder, the GTS values decreased by 22.09% after adding 9 wt.% ACSW and 8 wt.% polyester fiber. The negative influence of the ACSW and polyester fiber on the temperature sensitivity of the asphalt binders was related to their content levels. In detail, with the increase in polyester fiber contents, the GTS values of the APMAs gradually decreased under 9 wt.% ACSW, and the GTS values of the APMAs first increased and then decreased under 11 wt.% ACSW; meanwhile, the GTS values of the APMAs first decreased and then increased under 13 wt.% ACSW. By increasing the ACSW contents, the GTS values of the APMAs gradually

decreased under 4 wt.% polyester fiber; the *GTS* values of the APMAs first increased and then decreased under 6 wt.% polyester fiber, and the *GTS* values of the APMAs gradually increased under 8 wt.% polyester fiber, respectively. Furthermore, the *GTS* results additionally verified that the ACSW and polyester fiber could remarkably reduce the high-temperature fluidity of the asphalt binder.

3.2.3. The Results of $G^*/\sin\delta$

The impact of the ACSW and polyester fiber on the anti-deformation property of the asphalt binder was researched using the rutting factor ($G^*/\sin\delta$) and the larger the value of $G^*/\sin\delta$, the greater the anti-deformation of the APMA. The $G^*/\sin\delta$ values of the asphalt binder modified with and without the ACSW and polyester fiber under different temperatures are shown in Figure 5.

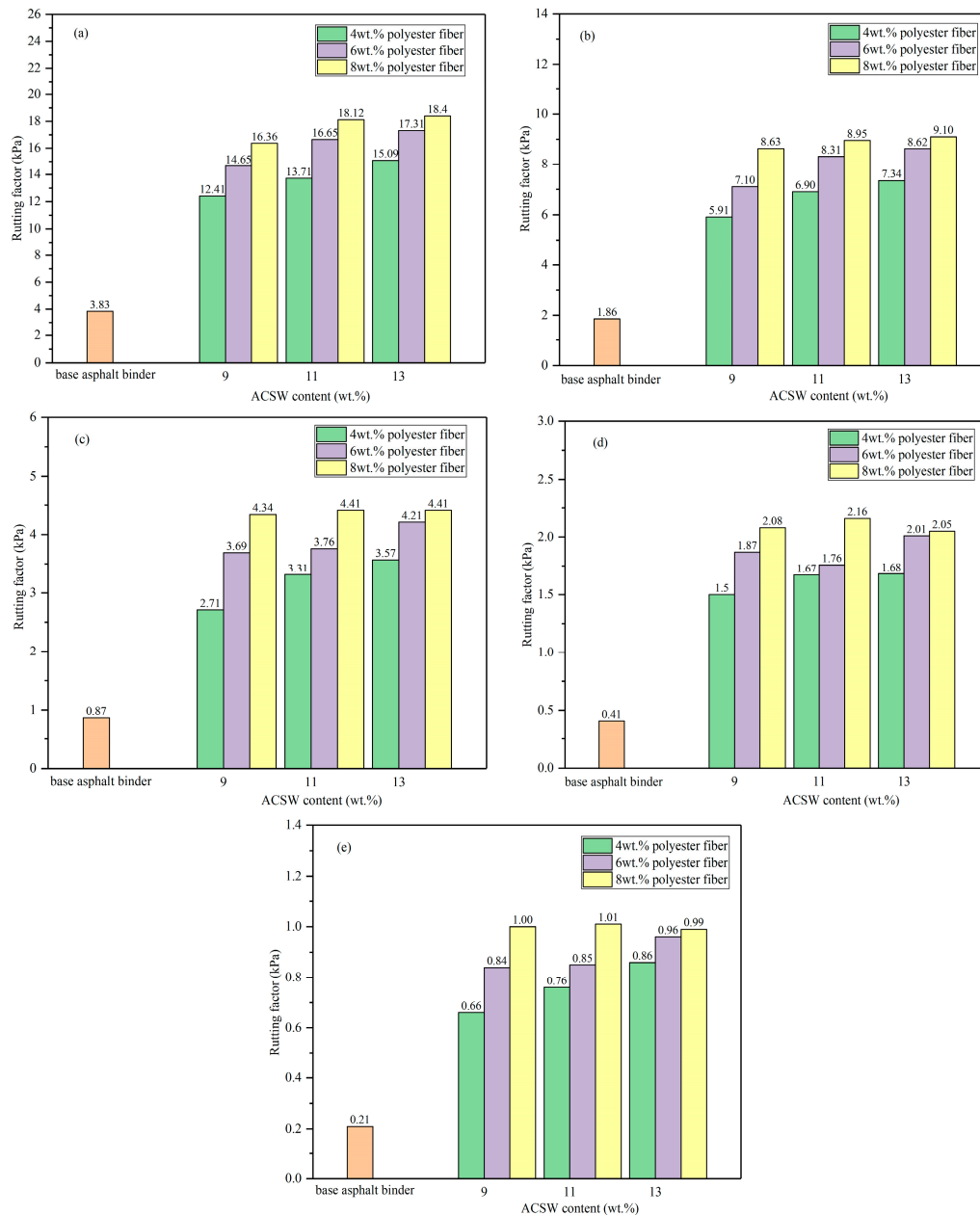


Figure 5. Rutting factor results of the APMAs under different temperatures. (a) 58 °C; (b) 64 °C; (c) 70 °C; (d) 76 °C; and (e) 82 °C.

From Figure 5, it could be seen that, when the temperatures were changed from 58 °C to 82 °C, the $G^*/\sin\delta$ values of the APMAs sharply decreased. At the same temperature, the $G^*/\sin\delta$ value of the base asphalt binder was lower than those of the APMAs. The results evaluated that the ACSW and polyester fiber-compound modification would obviously enhance the anti-deformation of the asphalt binder. The reasons behind this phenomenon might include the following two aspects: firstly, raising the temperature reduced the friction between the asphalt components; and secondly, when the temperature was constant, the movement of the light components of the asphalt binder was restricted by the adsorption and reinforcement behavior of the ACSW and polyester fiber.

3.2.4. Failure Temperature

A failure temperature was adopted to characterize the grade of high-temperature anti-deformation of the APMAs. Based on the Strategic Highway Research Program (SHRP), the $G^*/\sin\delta$ value needs to be greater than 1.0 kPa. Therefore, the temperature corresponding to the $G^*/\sin\delta$ value equal to 1.0 kPa was referred to as the failure temperature in this paper. The linear regression equation between $G^*/\sin\delta$ and temperature was executed according to Equation (3), and the results of the failure temperature of the APMAs were calculated as listed in Table 4.

$$\lg(G^*/\sin\delta \times 10^3) = a + b \times T \quad (3)$$

where a and b are the regression coefficients.

Table 4. Failure temperature of the APMAs.

ACSW Content (wt.%)	0	9	9	9	11	11	11	13	13	13
Polyester fiber content (wt.%)	0	4	6	8	4	6	8	4	6	8
Failure temperature (°C)	68.9	78.8	80.9	82.2	80.0	80.7	82.2	81.0	82.0	81.9

From Table 4, it could be seen that the failure temperature values of the APMAs were larger than that of the base asphalt binder; meanwhile, the failure temperature of all the APMAs was higher than 70 °C. When the content of the ACSW was 11 wt.% and that of the polyester fiber was 8 wt.%, the failure temperature of the APMA reached its maximum value (82.2 °C), and it was 19.3% larger than that of the base asphalt binder (68.9 °C).

Combining the results of the Brookfield rotational viscosity test and the DSR test, the ACSW and polyester fiber-compound modification had an obvious enhancement in the temperature-sensitivity and high-temperature anti-deformation of the asphalt binder, and this finding was consistent with the references [15,16]. The optimal contents of the APMA with better high-temperature rheological characteristics were 11 wt.% ACSW and 8 wt.% polyester fiber.

3.3. Low-Temperature Property

3.3.1. The Results of the BBR Test

The influence of the ACSW and polyester fiber on the low-temperature property of the asphalt binder was analyzed using the BBR test. According to AASHTO M313 [28], the creep stiffness (S) value needs to be less than 300 MPa, and the m -value needs to be larger than 0.3. The results of the BBR test of the APMAs at −12 °C are shown in Figures 6 and 7.

The low-temperature anti-deformation property of the asphalt binder was evaluated using the S -values. The lower the S -values, the better the low-temperature anti-deformation property of the modified asphalt binders. From Figure 6, the S -values of the APMAs were larger than that of the base asphalt binder (126.9 MPa), and, with the content levels of the ACSW and polyester fiber increased, the S -values of the APMAs first increased and then decreased. The S -values of all the APMAs were lower than 300 MPa. Detailed discussions were as follows: When the content of ACSW was 13 wt.% and the polyester fiber content was 6 wt.%, the S -value of the APMA reached its maximum value (252.6 MPa) and was

99.1% larger than that of the base asphalt binder (126.9 MPa). After adding the ACSW and polyester fiber, the consistency of the asphalt binder increased and a reinforced structure was formed inside the APMA, which would make the asphalt's binder property brittle. When the amounts of ACSW and polyester fiber exceeded a certain range, the *S* value of the APMA was reduced. The reason for this might be that the light components of the asphalt binder could not be fully absorbed by the surface of the ACSW and polyester fiber; meanwhile, the polyester fiber was gathered in the asphalt binder's structure, where the stress was weak [33].

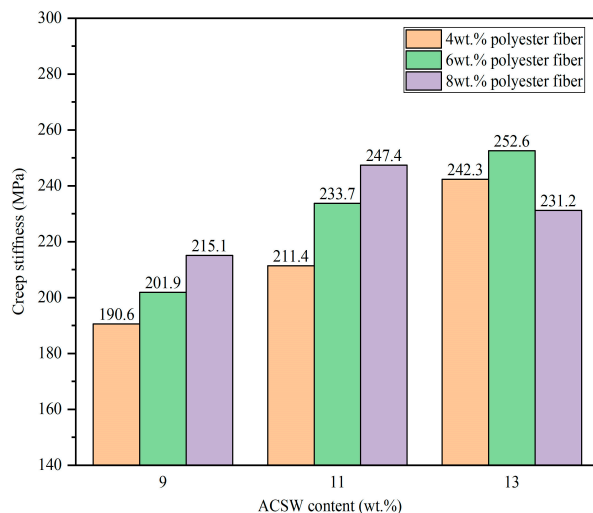


Figure 6. Creep stiffness results of the APMAs.

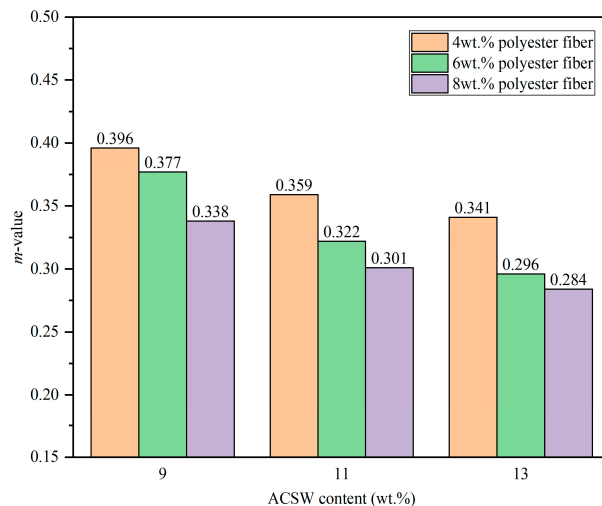


Figure 7. *m*-value results of the APMAs.

The *m*-value referred to the change rate of the stiffness modulus for the asphalt binder with test time and expressed the stress dissipation level of the asphalt binder. The larger the *m*-value, the faster the stress scattered and disappeared from the asphalt binder.

It can be seen from Figure 7 that the *m*-value of the asphalt binder was reduced after adding the ACSW and polyester fiber. At the same content level of ACSW (or polyester fiber), the *m*-value of the APMAs gradually decreased with the increasing in the contents of polyester fiber (or ACSW). When the contents of ACSW were not higher than 11 wt.%, the *m*-value of all the APMAs was larger than 0.3; meanwhile, when the content of ACSW was 13 wt.%, the *m*-value of the APMA was 0.296, and it was 0.284 under 6 wt.% and 8 wt.% polyester fiber, respectively. Compared to the base asphalt binder (0.448 *m*-value),

the *m*-value of the asphalt binder modified with 13 wt.% ACSW and 6 wt.% polyester fiber or 13 wt.% ACSW and 8 wt.% polyester fiber was decreased by 33.93% and 36.61%. This result suggested that adding the ACSW and polyester fiber reduced the low-temperature performance of the asphalt binder, possibly because the ACSW and polyester fiber declined the stress scatter and disappear energy of the asphalt binder at low temperatures.

3.3.2. The Results of the Force Ductility Test

The maximum tension and tensile work (namely, envelop area of tension elongation curve) were adopted to research the low-temperature characteristic of the APMAs. The results of the force ductility test are shown in Figures 8 and 9. The values of the maximum tension and tensile work of the base asphalt binder were 55.4 N and 0.130 J, respectively.

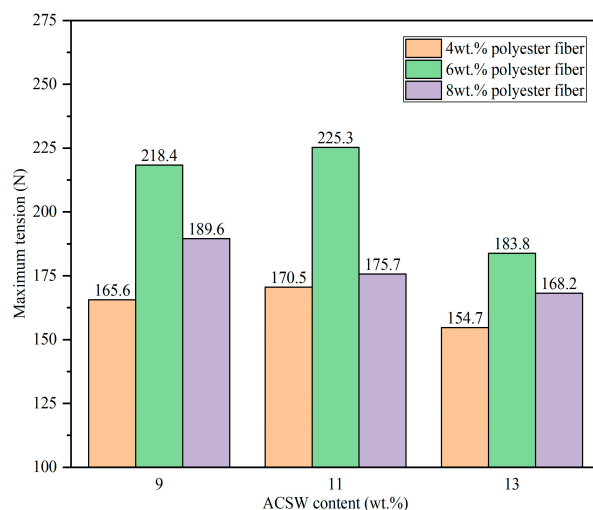


Figure 8. Maximum tension results of the APMAs.

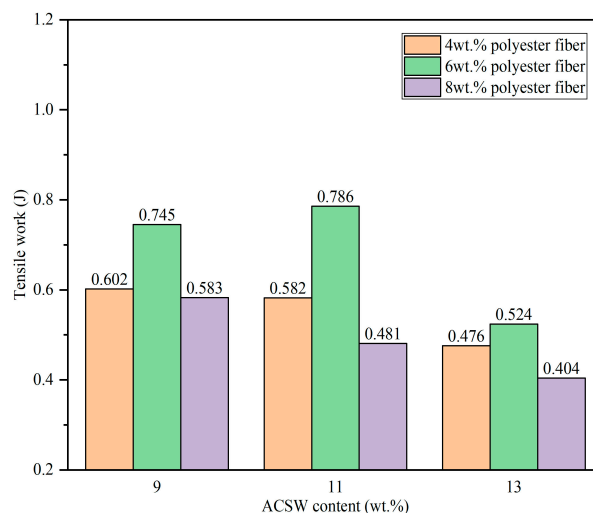


Figure 9. Tensile work results of the APMAs.

The maximum tension represented the tensile cohesive failure strength of the asphalt binder when it entered the yield stage. The larger the value of maximum tension, the greater the low-temperature characteristic of the APMA. From Figure 8, the maximum tension values of the asphalt binder sharply increased with the addition of the ACSW and polyester fiber. The results indicated that the tensile force required for the asphalt binder to enter the yield stage increased after adding the ACSW and polyester fiber; namely, the ACSW and polyester fiber could enhance the low-temperature ability of the asphalt binder. Under the

same contents of ACSW, the maximum tension values of the APMAs first increased and then decreased by increasing the contents of polyester fiber. When the dosage levels of the polyester fiber were 4 wt.% and 6 wt.%, respectively, the maximum tension values of the APMAs were, first, gradually enhanced and then decreased by increasing the dosage of ACSW, and, when the dosage level of the polyester fiber was 8 wt.%, the maximum tension values of the APMAs became lower by increasing the dosage of ACSW. After adding 11 wt.% ACSW and 6 wt.% polyester fiber, the maximum tension of the APMA reached its maximum value (225.3 N) and was 3.1 times larger than that of the base asphalt binder (55.4 N). This result implied that adding the ACSW and polyester fiber greatly enhanced the tensile cohesive failure strength of the asphalt binder, possibly because the ACSW and polyester fiber provided a three-dimensional interwoven mesh structure within the asphalt binder structure [15,33].

The tensile work comprehensively considered the change of tensile force and elongation during the force ductility test. The larger the value of tensile work, the greater the low-temperature ductility of the APMA. From Figure 9, the values of the tensile work of the APMAs were larger than that of the base asphalt binder (0.130 J). When the dosage levels of the ACSW were constant, the tensile work values of the asphalt binder increased at first and then decreased by increasing the content of polyester fiber. After mixing with 6 wt.% polyester fiber, the tensile work value of the asphalt binder was gradually larger at first and then lower with the increased dosage of ACSW, and, when the dosage level of the polyester fiber was 4 wt.% and 8 wt.%, respectively, the tensile work value of the APMAs became lower by increasing the dosage of ACSW. After adding 11 wt.% ACSW and 6 wt.% polyester fiber, the tensile work of the APMA reached its maximum value (0.786 J), and it was 5.05 times greater than that of the base asphalt binder (0.130 J). This result suggested that adding the ACSW and polyester fiber greatly improved the low-temperature tensile work for the asphalt binder. The reason behind this might be that the fiber-modified asphalt binder would be considered as a fiber-composite-reinforced material with asphalt binder as the matrix. The fiber produced a marked effect in strengthening the asphalt binder structure through “adsorption” and “interlacing” behaviors. During the tensile process of the fiber-modified asphalt binder, the three-dimensional, randomly distributed fibers inside the structure consumed the tensile stress and gradually shifted in the direction of the tensile force. At the same time, the interface friction between the asphalt binder and the fibers prevented the asphalt binder from moving along the tensile direction. Therefore, when the contents of ACSW and polyester fiber were appropriate, they gave full play to the above-described strengthening effect in the asphalt binder. However, when the contents of ACSW and polyester fiber were excessive, an effective interface layer could not be formed between the asphalt binder and the surface of the ACSW and polyester fiber and the ACSW and polyester fiber were made to easily aggregate in the asphalt binder. The reduction in the maximum tension and tensile work of the APMA led to weak areas with defects appearing in the asphalt binder.

Comparing the results of the BBR test and the force ductility test, there was a deviation between the two tests in evaluating the low-temperature characteristic of the APMAs. Previous researchers found that the conclusions obtained using the BBR test to study the low-temperature characteristic of fiber-modified asphalt were sometimes inconsistent with the results of a fiber-modified asphalt mixture. This might be because, during the BBR test, the upper load change of the beam specimen is usually ignored and the stiffness modulus of the specimen is mainly dependent on the mid-span deflection value of the specimen. According to the data recorded in the test process, the mid-span deflection of the APMA specimen was small at the end of the test, and it could not effectively reflect the “interlacing” reinforcement effect of the ACSW and polyester fiber in the asphalt binder structure. Therefore, the force ductility test was more suitable for evaluating the low-temperature performance of the APMA.

3.4. Microscopic Characterization

As shown in Figure 10, it was obvious that the FTIR spectra of the base asphalt binder, polyester fiber modified asphalt, ACSW modified asphalt, and APMAs showed almost the same absorption bands. In detail, the absorption bands at 2916.6 cm^{-1} and 2850.3 cm^{-1} were attributed to the symmetric and asymmetric vibration of methylene ($-\text{CH}_2$). The bands at 1456.0 cm^{-1} and 1375.5 cm^{-1} were ascribed to the hypo-methyl ($-\text{CH}$) in-plane stretching vibration of methyl ($-\text{CH}_3$) and methylene. The bands at 1153.2 cm^{-1} and 1031.2 cm^{-1} were owed to the vibration of sulfonyl ($\text{S}=\text{O}$) and implied that the thermal oxidation aging of the asphalt binder was generated during the processes of production and transportation. The bands at $900\text{--}700\text{ cm}^{-1}$ were ascribed to the bending vibrations of the hypo-methyl in aromatics. The results of the FTIR test evaluated that no new functional groups were generated, namely, that the preparing process of the APMA was one involving physical blending.

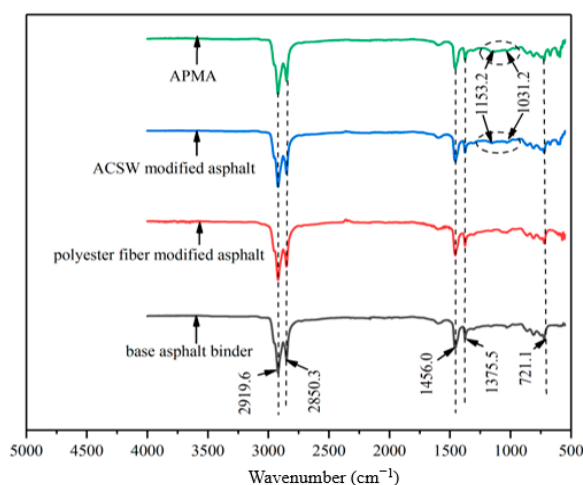


Figure 10. FTIR spectra of the APMAs.

The micro-structure of the asphalt binder with the ACSW and polyester fiber are shown in Figure 11. There were mainly physical adsorption and interweaving between the asphalt binder and the ACSW-polyester fiber. The light fractions of the asphalt binder were soaked up on the surface of the ACSW and polyester fiber, producing a larger interfacial bonding force between the asphalt binder and the ACSW-polyester fiber. In addition, the three-dimensional random dispersion of the polyester fiber formed a network in the asphalt binder to enhance its properties. This finding illustrated the previous experimental results from a microscopic perspective; namely, the ACSW and polyester fiber could strengthen the viscosity, anti-deformation, and low-temperature characteristics of the asphalt binder.

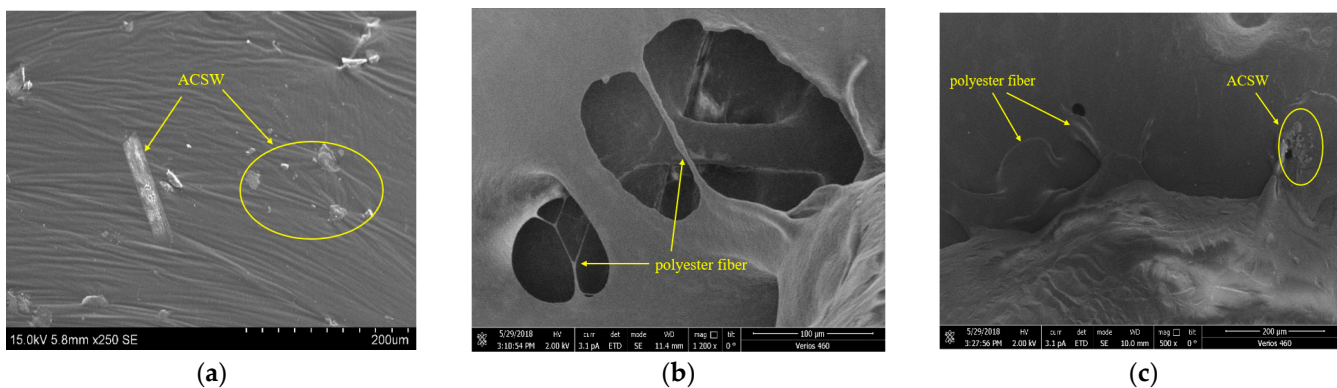


Figure 11. SEM images of the AMPAs. (a) ACSW-modified asphalt; (b) polyester fiber-modified asphalt; and (c) AMPA.

4. Conclusions

This research investigated the feasibility of using calcium sulfate anhydrous whiskers (ACSW) and polyester fibers to enhance the properties of asphalt binders. The results promote the application of ACSWs in asphalt pavement materials and effectively reduce the environmental pollution caused by calcium salt and gypsum. The conclusions are as follows:

1. The *VTS* and *GTS* values of the compound-modified asphalt binder decreased by 12.7% and 20.65% after adding 11 wt.% ACSW and 8 wt.% polyester fiber, compared to the base asphalt binder. ACSWs and polyester fibers could improve the viscosity-temperature and temperature-sensitivity performances of asphalt binders.
2. The viscosity and rutting factor of the modified asphalt binder were significantly enhanced compared to the base asphalt binder, which suggested that ACSW and polyester fiber could improve the high-temperature anti-deformation characteristics of asphalt binders.
3. The force ductility test was more suitable than the BBR test for evaluating the low-temperature performance of the ACSW and polyester fiber-composite-modified asphalt binder. The maximum tension and tensile work of the asphalt binder modified with 11 wt.% ACSW and 6 wt.% polyester fiber increased by 3.1 times and 5.05 times, respectively, compared to the base asphalt binder. In addition, the influence of ACSWs and polyester fibers on the low-temperature ability of asphalt binders needs to be further considered in combination with its influence on the asphalt mixtures in question.
4. The effect of the ACSW and polyester fiber on the characteristics of the asphalt binders was related to their contents. When the ACSW content was 11 wt.% and the polyester fiber contents were 6 wt.%~8 wt.%, the better properties of the ACSW and polyester fiber-composite-modified asphalt binder were obtained.
5. There was mainly a physical interaction and interleaving process between the ACSW-polyester fiber and the base asphalt binder in the preparing process of the ACSW and polyester fiber-composite-modified asphalt binder.

Author Contributions: Funding acquisition, C.S.; investigation, T.F.; methodology, T.F.; writing—original draft, T.F.; writing—review and editing, C.S. and J.G. All authors have read and agreed to the published version of the manuscript.

Funding: This study is financially supported by the National Natural Science Foundation of China (11972237, 52378455), the Key R&D Project of Hebei Province (21373801D), the Science and Technology Project of Hebei Education Department (QN2023178), and the Project of Hebei Provincial Department of Transportation (JD-202007).

Institutional Review Board Statement: Not applicable.

Informed Consent Statement: Not applicable.

Data Availability Statement: Data sharing not applicable. No new data were created or analyzed in this study.

Conflicts of Interest: The authors declare no conflict of interest.

References

1. Li, J.; Zhuang, X.G.; Querol, X.; Font, O.; Moreno, N. A review on the applications of coal combustion products in China. *Int. Geol. Rev.* **2018**, *60*, 671–716. [[CrossRef](#)]
2. Chen, S.H.; Liu, Q.; He, X.Y.; Su, Y.; Zhang, B.; Xu, H. One-step synthesis of nanoscale anhydrous calcium sulfate whiskers: Direct conversion of calcium carbonate by mixed acid with microemulsion method. *J. Nanopart. Res.* **2022**, *24*, 4. [[CrossRef](#)]
3. Zhou, D.; Wei, R.F.; Zhu, Y.L.; Long, H.M.; Huang, B.F.; Wang, Y.F.; Wu, S.H.C. Calcium sulfate whisker one-step preparation using semi-dry flue gas desulfurization ash and directional growth control. *J. Clean. Prod.* **2021**, *290*, 125754. [[CrossRef](#)]
4. Li, Q.B.; Liu, H.; Nie, C.H.; Xie, G.M.; Che, Z.H.M.; Zhu, D.H.; Guo, L.; Xiang, Y.; Shi, W. PMMA-Grafted calcium sulfate whiskers for applications as fillers in PVC. *Polymers* **2022**, *14*, 4199. [[CrossRef](#)] [[PubMed](#)]

5. Yang, J.N.; Nie, S.H.B.; Zhu, J.B. Fabrication and characterization of poly (lactic acid) biocomposites reinforced by calcium sulfate whisker. *J. Polym. Environ.* **2018**, *26*, 3458–3469. [[CrossRef](#)]
6. Chen, C.H.; Wang, Y.B.; Wang, H.; Deng, Q.Q.; Du, L.; Gao, G.S.H.; Luan, F.C.H. Effect of different kinds of CaSO₄ whisker on the bending strength and hygroscopicity of gypsum board. *Appl. Mech. Mater.* **2014**, *638*, 1322–1325. [[CrossRef](#)]
7. Yang, Y.R.; Zhang, Q.J.; Cai, W.; Yi, M.G.; Xiang, L. Formation and application of hierarchical calcium silicate-calcium sulfate whiskers. *Mater. Des.* **2018**, *146*, 172–179. [[CrossRef](#)]
8. Xu, L.; Fang, K.N.; Bi, Y.X.; Yang, M.; Chen, Q.L. Preparation of anhydrous micron CaSO₄ with different morphologies from phosphogypsum and its reinforcing in polyvinyl chloride. *Constr. Build. Mater.* **2023**, *365*, 130126. [[CrossRef](#)]
9. Lou, J.F.; Zhang, K.; Qin, S.H.H.; Lei, Y.; Liu, Y.F.; He, M.; Yu, J. Two-dimensional lamellar phosphogypsum/polyethylene glycol composite PCM: Fabrication and characterization. *J. Ind. Eng. Chem.* **2022**, *113*, 431–438.
10. Men, J.H.; Li, Y.M.; Cheng, P.F.; Zhang, Z.H.M. Recycling phosphogypsum in road construction materials and associated environmental considerations: A review. *Heliyon* **2022**, *8*, e11518. [[CrossRef](#)]
11. Cheng, X.W.; Dong, Q.G.; Li, Z.Y.; Guo, X.Y. High-temperature mechanical properties of CaSO₄ whiskers reinforced high alumina cement. *Mag. Concr. Res.* **2020**, *72*, 55–67. [[CrossRef](#)]
12. Cao, K.; Liu, G.G.; Li, H.; Huang, Z.H.Y. Mechanical properties and microstructure of calcium sulfate whisker-reinforced cement-based composites. *Materials* **2022**, *15*, 947. [[CrossRef](#)] [[PubMed](#)]
13. Xu, Y.; Xu, Y.L. Comparative Study on Pavement Performance of Asphalt Mixtures Modified by Calcium Sulfate Whisker and Calcium Carbonate Whisker. *Coatings* **2022**, *12*, 1513. [[CrossRef](#)]
14. Li, G.Y.; Li, J.F.; Gao, Y.; Liu, Y.Q. Research on temperature sensitivity and viscosity of calcium sulphate whisker modified asphalt. *New Chem. Mater.* **2017**, *45*, 235–237.
15. Fan, T.T.; Wang, X.S.H.; Gao, Y.; Zhang, X.Y. Investigating the interaction mechanism and effect of different calcium sulfate whiskers on performance of asphalt binder. *Constr. Build. Mater.* **2019**, *224*, 515–533. [[CrossRef](#)]
16. Fan, T.T.; Wang, X.S.H. Influence of calcium sulfate whisker on the high temperature performance of asphalt binder. *Pet. Sci. Technol.* **2020**, *38*, 303–308. [[CrossRef](#)]
17. Ye, Q.S.H.; Wu, S.P. Rheological properties of fiber reinforced asphalt binders. *Indian J. Eng. Mater. Sci.* **2009**, *16*, 93–99.
18. Yong, W.; Wang, Y. High-temperature rheological properties of asphalt binders with polymeric, warm-mix, and rubber particulate additives. *J. Mater. Civ. Eng.* **2019**, *31*, 04018404.
19. Xing, X.Y.; Pei, J.Z.H.; Shen, C.H.; Li, R.; Zhang, J.P.; Huang, J.Y.; Hu, D.L. Performance and reinforcement mechanism of modified asphalt binders with nano-particles, whiskers, and fibers. *Appl. Sci.* **2019**, *9*, 2995. [[CrossRef](#)]
20. Yousif, R.A.; Tayh, S.A.; Al-Saadi, I.F.; Jasim, A.F. Physical and Rheological Properties of Asphalt Binder Modified with Recycled Fibers. *Adv. Civ. Eng.* **2022**, *2022*, 1223467. [[CrossRef](#)]
21. Fu, Z.H.; Tang, Y.J.; Ma, F.; Wang, Y.J.; Shi, K.; Dai, J.S.H.; Hou, Y.J.; Li, J. Rheological properties of asphalt binder modified by nano-TiO₂/ZnO and basalt fiber. *Constr. Build. Mater.* **2022**, *320*, 126323. [[CrossRef](#)]
22. Liu, Y.T.; Yang, Z.L.; Luo, H. Experimental investigation of eco-friendly anhydrous calcium sulfate whisker and waste cooking oil compound modified asphalt mixture. *Materials* **2023**, *16*, 2409. [[CrossRef](#)] [[PubMed](#)]
23. Fan, T.T.; Song, Q.P.; Si, C.H.D.; Han, S.K. The multi-objective optimization design and hydrothermal performance evaluation of anhydrous calcium sulfate whisker and polyester fiber compound modified asphalt mixture in hot-humid areas. *Materials* **2023**, *16*, 6662. [[CrossRef](#)]
24. Arabani, M.; Shabani, A. Evaluation of the ceramic fiber modified asphalt binder. *Constr. Build. Mater.* **2019**, *205*, 377–386. [[CrossRef](#)]
25. Ma, F.; Jin, Y.X.; Fu, Z.H.; Dai, J.S.H.; Zhang, P.; Zhang, C.H.; Wen, Y.L. Influencing factors and evaluation methods of reinforcement effect of fiber-modified asphalt binder. *Polym. Compos.* **2022**, *43*, 8986–8999. [[CrossRef](#)]
26. ASTM D4402/4402M; Standard Test Method for Viscosity Determination of Asphalt at Elevated Temperatures Using a Rotational Viscometer. ASTM International: West Conshohocken, PA, USA, 2015.
27. AASHTO T315; Standard Method of Test for Determining the Rheological Properties of Asphalt Binder Using a Dynamic Shear Rheometer (DSR). American Association of State Highway and Transportation Officials: Washington, DC, USA, 2016.
28. AASHTO T313; Standard Method of Test for Determining the Flexural Creep Stiffness of Asphalt Binder Using the Bending Beam Rheometer (BBR). American Association of State Highway and Transportation Officials: Washington, DC, USA, 2009.
29. Pereira, L.; Freire, A.C.; da Costa, M.S.; Antunes, V.; Quaresma, L.; Micaelo, R. Experimental study of the effect of filler on the ductility of filler-bitumen mastics. *Constr. Build. Mater.* **2018**, *189*, 1045–1053. [[CrossRef](#)]
30. Bai, M. Investigation of low-temperature properties of recycling of aged SBS modified asphalt binder. *Constr. Build. Mater.* **2017**, *150*, 766–773. [[CrossRef](#)]
31. Rodríguez-Alloza, A.M.; Gallego, J.; Pérez, I. Study of the effect of four warm mix asphalt additives on bitumen modified with 15% crumb rubber. *Constr. Build. Mater.* **2013**, *43*, 300–308. [[CrossRef](#)]

32. Xie, X.B.; Li, M.D.; Liang, L.Y.; Tong, S.H.J.; Li, G.H. Evaluation index of low temperature rheological properties of asphalt mortar based on force ductility. *J. Mater. Sci. Eng.* **2022**, *40*, 491–498.
33. Fan, T.T.; Si, C.; Zhang, Y.; Zhu, Y.F.; Li, S. Optimization design of asphalt mixture composite reinforced with calcium sulfate anhydrous whisker and polyester fiber based on response surface methodology. *Materials* **2023**, *16*, 594. [[CrossRef](#)]

Disclaimer/Publisher’s Note: The statements, opinions and data contained in all publications are solely those of the individual author(s) and contributor(s) and not of MDPI and/or the editor(s). MDPI and/or the editor(s) disclaim responsibility for any injury to people or property resulting from any ideas, methods, instructions or products referred to in the content.